Infection and Drug Resistance

Dovepress
Taylor & Francis Group

Open Access Full Text Article

ORIGINAL RESEARCH

Doxycycline-Induced Apoptosis in *Brucella suis* S2-Infected HMC3 Cells via Calreticulin Suppression and Activation of the IRE1/Caspase-3 Signaling Pathway

Zhao Wang[1], Juan Yang[2], Deng-Er Zhang[3], Xia Qiao[4], Shu-Long Yang[5], Zhen-Hai Wang[2,6], Qian Yang[1]

[1]Department of Experimental Surgery, The Second Affiliated Hospital of Air Force Medical University, Xi'an, People's Republic of China; [2]Neurology Center, The General Hospital of Ningxia Medical University, Yinchuan, People's Republic of China; [3]The First Clinical Medical School, Ningxia Medical University, Yinchuan, People's Republic of China; [4]Institute of Medical Science, The General Hospital of Ningxia Medical University, Yinchuan, People's Republic of China; [5]Department of Orthopedics, The People's Hospital of Wuhai, Wuhai, People's Republic of China; [6]Diagnosis and Treatment Engineering Technology Research Center of Nervous System Diseases of Ningxia Hui Autonomous Region, The General Hospital of Ningxia Medical University, Yinchuan, People's Republic of China

Correspondence: Qian Yang, Department of Experimental Surgery, The Second Affiliated Hospital of Air Force Medical University, No. 569 of Xinsi Road, Baqiao District, Xi'an, 710032, People's Republic of China, Tel +86029-84777007, Email yangqianyqq@126.com; Zhen-Hai Wang, Neurology Center, The General Hospital of Ningxia Medical University, No. 804 of Shengli Street, Xingqing District, Yinchuan, 750003, People's Republic of China, Tel +860951-6744025, Email wangzhenhaiwzh01@126.com

Objective: This study aims to elucidate the apoptotic mechanism induced by doxycycline (Dox) in human microglial clone 3 (HMC3) cells infected with the *Brucella suis* S2 strain, with the goal of identifying potential therapeutic targets for neurobrucellosis.

Methods: The expression of calreticulin (CALR) at both the protein and mRNA levels was assessed using Western blot analysis and reverse transcription-quantitative polymerase chain reaction (RT-qPCR), respectively, following exposure of HMC3 cells to varying concentrations and treatment durations of Dox. Apoptosis rates were determined via flow cytometry. To investigate the involvement of the inositol-requiring enzyme-1 (IRE1)/Caspase-12/Caspase-3 pathway, CALR protein levels were analyzed through Western blot after a 12-hour treatment with 160 μM Dox. Endoplasmic reticulum (ER) stress and intracellular calcium (Ca^{2+}) concentrations were evaluated using fluorescent staining. The same parameters were measured in *B. suis* S2-infected HMC3 cells following treatment with 160 μM Dox.

Results: Treatment with 160 μM Dox for 12 hours resulted in a reduction in CALR protein levels and the induction of apoptosis in HMC3 cells. The downregulation of CALR activated the IRE1/Caspase-12/Caspase-3 signaling pathway, leading to apoptosis. Similar apoptotic effects were observed in *B. suis* S2-infected HMC3 cells following Dox treatment.

Conclusion: Dox promotes apoptosis in *B. suis* S2-infected HMC3 cells by suppressing CALR expression and activating the IRE1/Caspase-12/Caspase-3 signaling pathway. These findings suggest that CALR regulation may serve as a potential therapeutic target for neurobrucellosis.

Keywords: apoptosis, *Brucella suis* S2 strain, doxycycline, HMC3, IRE1/Caspase-12/Caspase-3 pathway

Introduction

Human brucellosis, caused by *Brucella* spp., is a zoonotic disease that can affect multiple organ systems.[1] In severe cases, patients may exhibit musculoskeletal or neurological complications.[2] Central nervous system (CNS) involvement frequently manifests as meningitis, encephalitis, brain abscesses, and demyelinating lesions.[3] Neurobrucellosis often results in chronic infections with an increased risk of recurrence, posing significant health risks.[4] These manifestations are closely associated with the role of microglia in CNS infections.[1]

Microglia, derived from erythromyeloid progenitor cells in the yolk sac, function as resident macrophages within the CNS.[5] They contribute to immune defense by secreting pro-inflammatory cytokines and chemokines, playing a crucial

Received: 18 November 2024
Accepted: 14 April 2025
Published: 23 April 2025

role in the clearance of dead neurons and the response to pathogenic infections.[6,7] Macrophages represent primary target cells for *Brucella*.[8] Within host macrophages, *Brucella* resides in membrane-bound compartments known as *Brucella*-containing vacuoles (BCVs), where it evades immune responses by preventing fusion with lysosomes. Additionally, *Brucella* interacts extensively with the endoplasmic reticulum (ER) to establish a vacuolar niche conducive to intracellular replication.[9] During this process, *Brucella* can inhibit apoptosis to facilitate persistent infection.[8] However, the molecular mechanisms underlying Brucella-mediated regulation of microglial apoptosis through ER interactions remain largely unexplored.

The ER is critical for protein synthesis and processing, lipid metabolism, and calcium homeostasis.[10] Bacterial infections can induce ER stress, characterized by the accumulation of misfolded or unfolded proteins.[11] *Brucella* establishes intracellular infections, in part, by modulating ER stress-mediated apoptosis.[12] To mitigate ER stress, host cells activate the unfolded protein response (UPR), which involves three key receptors: inositol-requiring enzyme-1 (IRE1), PKR-like ER kinase (PERK), and activating transcription factor-6 (ATF6).[11] Among these, IRE1 represents the most evolutionarily conserved UPR signaling pathway and plays a pivotal role in *Brucella*-induced, ER stress-associated apoptosis.[13] Caspase-12, a key regulator of ER stress-induced apoptosis,[14] is activated through IRE1 and subsequently triggers downstream apoptotic effectors, including Caspase-9 and Caspase-3.[15]

Calreticulin (CALR), a multifunctional chaperone protein primarily localized in the ER regulates ER stress by maintaining calcium homeostasis.[16] Additionally, CALR has been implicated in apoptosis regulation in bacterially infected microglia.[17] Previous studies have demonstrated that *Brucella suis* S2 strain inhibits apoptosis in human microglial clone 3 (HMC3) cells by increasing CALR expression.[18,19] *B. suis* S2, a live vaccine strain that underwent spontaneous attenuation, was first isolated in 1952 from the fetus of an aborted pig.[20,21] Its virulence in humans is evidenced by symptoms such as fatigue and excessive perspiration in infected individuals.[21] In addition to preventing host cell apoptosis, *B. suis* S2 suppresses the host inflammatory response by inhibiting the NF-κB signaling pathway and the NLRP3 inflammasome, thereby promoting its long-term survival within host cells.[21–23] However, the relationship between CALR levels and apoptosis mediated by the IRE1α/Caspase-12/Caspase-3 pathway in *Brucella*-infected microglia remains unexplored. Given these molecular interactions, further investigation into the effects of antibiotic treatment on apoptosis in *Brucella*-infected microglia is warranted.

Doxycycline (Dox), a second-generation tetracycline antibiotic, exhibits broad-spectrum antibacterial activity against both Gram-positive and Gram-negative bacteria and is well tolerated in clinical use.[24] As a result, Dox is recommended as the preferred treatment for chronic brucellosis and neurobrucellosis.[25] In addition to its antibacterial properties, Dox exerts non-antibiotic effects, including apoptosis induction, anti-inflammatory activity, and immunosuppressive properties.[26,27] Recent studies have highlighted the role of Dox in activating the caspase family cascade to induce apoptosis, as well as its capacity to act as an ER stress inducer.[27,28] However, the regulatory effect of Dox on ER stress-related apoptosis in *Brucella*-infected microglia remains largely unexplored.

In this study, HMC3 cells were treated with varying concentrations of Dox for different durations to determine the optimal conditions for apoptosis induction. Subsequently, Dox was administered to normal HMC3 cells, as well as CALR knockdown and overexpression cell lines, to assess its ability to induce apoptosis via the IRE1/Caspase-12/Caspase-3 pathway through CALR suppression. Based on these findings, it was concluded that Dox induces apoptosis in *B. suis* S2-infected HMC3 cells through a similar mechanism.

Materials and Methods

Antibodies and Lentivirus

Primary antibodies against phosphorylated inositol-requiring enzyme-1 (p-IRE1; Ser724, #GR271918-30), cleaved-Caspase-3 (#GR297363-10), cleaved-Caspase-12 (#GR3306653-9), GAPDH (#GR200347-16), and CALR (#GR3252549-6) were obtained from Abcam (Cambridge, UK). Primary antibodies against IRE1 (#I09262562), and cleaved-Caspase9 (#I05053421) were purchased from Wanlei Biotechnology (Shenyang, CHN). IRDye® 800CW-labeled goat anti-rabbit IgG (#C81210-05) was purchased from Li-COR (Lincoln, USA). CALR and sh-CALR lentivirus were acquired from Hanbio Biotechnology (Shanghai, CHN).

Cell Culture

HMC3 cells were obtained from Kelei Biotechnology (Shanghai, CHN) and authenticated using short tandem repeat (STR) profiling. Cells were maintained in complete Dulbecco's modified Eagle medium (DMEM; Gibco, Shanghai, CHN) supplemented with 12% fetal bovine serum (FBS; Gibco, Grand Island, USA) and 1% penicillin streptomycin (Solarbio, Beijing, CHN). Cultures were incubated at 37 °C in a humidified atmosphere containing 5% CO_2. Upon reaching 70% confluency in 10 cm dishes, HMC3 cells were washed twice with phosphate-buffered saline (PBS; Hyclone, Shanghai, China) and subcultured at a 1:4 ratio.

Bacteria

The *B. suis* S2 strain was preserved at the Ningxia Clinical Pathogenic Microorganisms Laboratory (Yinchuan, CHN). The strain was resuscitated and incubated in tryptic soy broth (TSB; Hope Biotech, Qingdao, China) at 35 °C with 5% CO_2 for 3–4 days. Single colonies were subsequently selected and transferred to 10 mL of TSB, followed by incubation in a rotary shaker at 180 rpm and 37 °C for 48 hours. The bacterial culture was then harvested by centrifugation at 4500 rpm for 5 minutes, washed twice with PBS, and resuspended. The bacterial density was determined using turbidimetry. All experiments involving *B. suis* S2 were conducted in a Biosafety Level 2 (BSL-2) facility at the Ningxia Clinical Pathogenic Microorganisms Laboratory, adhering strictly to laboratory biosafety regulations.

In vitro Bacterial Infection Experiments

HMC3 cells were seeded at a density of 2.5×10^5 cells per 10 cm dish in an antibiotic-free culture medium. Following a previously established protocol, cells were infected with *B. suis* S2 at a multiplicity of infection (MOI) of 50 for 2 hours, until reaching 70% confluence. Subsequently, cells were washed three times with cold PBS to remove extracellular *B. suis* S2 and collected for further experiments.

In vitro Dox Treatment

Dox (MedChem Express, Monmouth Junction, USA) was dissolved in PBS to prepare a 10 mm stock concentration and stored at −80 °C. For experimental treatments, Dox was diluted to the required concentrations in the culture medium. Upon reaching 70% confluence, HMC3 cells were exposed to 40 μM Dox for different durations (6, 12, and 24 hours).[29] Additionally, a separate set of HMC3 cells was treated with varying concentrations of Dox (20, 40, 80, and 160 μM) for 12 hours.[30] Furthermore, HMC3, HMC3-CALR, and HMC3-sh-CALR cell lines were treated with 160 μM Dox for 12 hours. *B. suis* S2-infected HMC3 cells were also exposed to 160 μM Dox for 12 hours.

Intracellular Colony Counting

Cells from each experimental group were collected and centrifuged at 1000 rpm for 5 minutes, followed by two washes with PBS to remove any extracellular *B. suis* S2. To lyse the cells, a 0.1% Triton X-100 solution was applied for 10 minutes at room temperature, followed by vortexing for 10 seconds. The lysates were subsequently diluted 100-fold in PBS, and 100 μL of the diluted samples were plated onto TSB agar using sterile applicator sticks. The plates were incubated at 37 °C for 3 to 4 days, after which colony-forming units (CFU) were counted. The number of intracellular bacteria (CFU/mL) was calculated using the formula: (number of colonies × dilution factor) / 0.1 mL.

Western Blot Analysis

HMC3 cell lines were seeded into 10 cm culture dishes at a density of 1×10^6 cells per dish in complete culture medium. After the cells reached approximately 85% confluence, protein expression levels of CALR, IRE1/p-IRE1, cleaved Caspase-12, cleaved Caspase-3, and cleaved Caspase-9 were analyzed using Western blotting. Cells were detached via trypsinization, collected by centrifugation at 1000 rpm for 5 minutes, and lysed for total protein extraction following the manufacturer's instructions (Whole Protein Extraction Kit, KeyGEN, Nanjing, China). The lysates were centrifuged at 13,500 rpm for 40 minutes at 4 °C, and protein concentrations were determined using the bicinchoninic acid (BCA) Protein Quantification Kit (KeyGEN, Nanjing, China).

Protein lysates (80 μg per lane) were diluted in 5× sodium dodecyl sulfate (SDS) loading buffer and denatured in a metal bath at 100 °C for 5 minutes. Proteins were then separated on 8–12% SDS-polyacrylamide gels (SDS-PAGE; KeyGEN, Nanjing, China) and transferred onto 0.45 μm polyvinylidene difluoride (PVDF) membranes (Millipore, Billerica, USA) via electrotransfer.

To block non-specific binding, membranes were incubated with 5% (w/v) nonfat milk in Tris-buffered saline containing 0.1% Tween-20 (TBST) for 2 hours at room temperature. Membranes were then incubated overnight at 4 °C with primary antibodies (dilution 1:500–1:1000), followed by five washes with TBST (5 minutes per wash).

Next, membranes were incubated with IRDye® 800CW Goat anti-Rabbit IgG (1:7500; LI-COR, Lincoln, USA) at 37 °C for 1 hour. Target proteins were detected and analyzed using the Odyssey Infrared Imaging System (LI-COR, Lincoln, USA).

Experiments were independently repeated three times. The mean optical density (MOD) of each target protein was quantified and normalized to GAPDH expression to determine relative protein levels.

Quantitative Real-Time PCR

HMC3 cell lines were seeded into 6 cm culture dishes at a density of 1×10^5 cells per dish and subjected to Dox treatment or *B. suis* S2 infection upon reaching 70% confluence. Total RNA from each group was extracted using the RNA simple Total RNA Kit (TIANGEN, Beijing, CHN) and reverse-transcribed into cDNA using the Transcriptor First Strand cDNA Synthesis Kit (Thermo Fisher Scientific, Waltham, USA). Primers for *CALR* and *GAPDH* were synthesized by Sangon Biotech (Shanghai, CHN) with the following sequences: *CALR*, Fwd-5′ CCAACGATGAGGCATACGCTGAG 3′, Rev-5′ GCTCCTCGTCCTGTTT-GTCCTTC 3′; *GAPDH*, Fwd-5′′ CAAGGTCATCCATGACAACTTTG 3′, Rev-5′ GTCCACCACCCTGTTGCTGTAG 3′. Primer reaction specificity was verified by melting curve and agarose gel analyses. qPCR analysis was conducted using the LightCycler® 480 II Authorized Thermal Cycler (Roche, Basel, Switzerland) and the ChamQ SYBR qPCR Master Mix (Vazyme Biotech, Nanjing, CHN). The amplification conditions were set as follows: initial denaturation at 95 °C for 30 seconds, followed by 40 cycles of amplification at 95 °C for 10 seconds, 56 °C for 30 seconds, and 72 °C for 30 seconds. Dissolution curve analysis was performed at 95 °C for 15 seconds, 60 °C for 60 seconds, and 95 °C for 15 seconds. The melting temperatures (Tm) of the Calr and Gapdh amplicons were expected to be 84.5 °C. All RT-qPCR experiments were independently repeated at least four times. The relative mRNA expression levels of Calr was quantified using the $2^{-\Delta\Delta CT}$ CT method, with Gapdh serving as the internal reference.

Flow Cytometry Analysis

Annexin V-FITC/PI Analysis

Apoptotic HMC3 cells induced by Dox were stained using a BBcellProbe™ Annexin V-FITC/PI staining kit (BestBio, Shanghai, CHN). Dox-treated cells were digested with trypsin (without EDTA) and collected. The cells were then washed twice with 2 mL of pre-cooled PBS and resuspended in 400 μL of Annexin V binding buffer at a density of 1×10^6 cells/mL. Subsequently, 5 μL of Annexin V-FITC staining solution was added to the cell suspension, which was protected from light and incubated at 4 °C for 15 minutes. Finally, 10 μL of propidium iodide (PI) solution was added to the suspension. Following a 5-minute incubation, a flow cytometer (BD Biosciences, San Jose, USA) was used to assess and quantify the apoptotic rate (%) of HMC3 cells in each experimental group.

Annexin V-APC/7-AAD Analysis

To prevent interference from the green fluorescence of the ZsGreen protein in Annexin V-FITC/PI analysis, the Annexin V-APC/7-AAD Apoptosis Kit (US Everbright, Suzhou, China) was employed to assess apoptosis in each HMC3 cell line. Single-cell suspensions were prepared in accordance with the methodology outlined in Annexin V-FITC/PI Analysis. Annexin V-APC (5 μL) and 7-AAD staining solution (10 μL) were added to each 100 μL cell suspension, and the mixtures were incubated for 15 minutes at room temperature, protected from light. Immediately afterward, 400 μL of Annexin V binding buffer was added to each cell mixture (approximately 4×10^5 cells), and the apoptotic rate was determined by flow cytometry analysis.

Results Analysis

Flow cytometry data were analyzed using FlowJo V10 software, with compensation performed using single-stained controls. The gating strategy was based on the control HMC3 cells. Cells in the Q1, Q2, Q3, and Q4 quadrants corresponded to necrotic, late apoptotic, early apoptotic, and viable cells, respectively. In this study, the apoptosis level in each group was calculated as the sum of the Q2 and Q3 quadrants.

ER Staining

HMC3 cell lines were seeded onto round coverslips in 12-well plates at a density of 2×10^5 cells/well. Each well was supplemented with 1 mL of complete medium, and the cells were incubated at 37 °C within 5% CO_2. Upon reaching 70% confluence, cells were treated with Dox or infected with *B. suis* S2. Subsequently, ER staining was performed following the manufacturer's instructions for the Endoplasmic Reticulum Staining Kit-Red Fluorescence (BestBio, Shanghai, China).

The BBcellProbe® E04 fluorescent dye was initially diluted 10-fold from the standard solution and then further diluted 20-fold with Hank's Balanced Salt Solution (HBSS; MeilunBio, Dalian, China) to prepare the working solution. Immediately afterwards, cells were washed twice with pre-warmed HBSS and stained with 1 mL of pre-heated working solution at 37 °C for 30 minutes in the dark. Cells were then fixed with 500 μL of 4% paraformaldehyde for 2 minutes and washed twice with pre-warmed HBSS. Finally, nuclei were stained using DAPI, and the coverslips were sealed with an anti-fade reagent to prevent fluorescence quenching. ER staining in each experimental group was observed and imaged using an FV1000 laser confocal microscope (Olympus, Tokyo, Japan).

Measurements of the Intracellular Calcium Ion Concentration

Each HMC3 cell line was seeded into 96-well plates at a density of 2×10^4 cells/well, with six replicate wells per group. The cell lines were placed in an incubator at 37 °C with 5% CO_2. When the cells reached 70% confluency, they were treated with Dox or infected with *B. suis* S2. Intracellular Ca^{2+} levels were subsequently assessed using the Intracellular Calcium Staining Kit (red fluorescence; BestBio, Shanghai, CHN).

The BBcellProbe® F07 fluorescent dye was diluted 500-fold in HBSS to prepare the staining working solution, which was added to each well. Cells were incubated for 50 minutes at 37 °C, followed by three washes with pre-warmed HBSS for 5 minutes each. Subsequently, 100 μL of HBSS was added to each well, and the cells were incubated for 30 minutes at 37 °C. The fluorescence intensity of intracellular Ca^{2+} was detected using a fluorescence microplate reader (BioTek, Winooski, Vermont, USA).

Statistical Analysis

At least three biologically independent replicates were performed for each experiment, and the results were expressed as mean ± standard deviation (SD). Statistical analysis of all experimental data was conducted using GraphPad Prism 8.0.2 software. The normality of the grouped data was assessed using the Shapiro–Wilk normality test, while homoscedasticity was evaluated using the Brown-Forsythe test. Differences among groups were analyzed by one-way analysis of variance (ANOVA). Throughout the study, p-values ≤ 0.05 were considered indicative of statistically significant differences between groups.

Results

The Impact of Dox on CALR Expression and Apoptosis in HMC3 Cells at Different Time Intervals

To examine the effects of different durations of Dox treatment on CALR expression and apoptosis in HMC3 cells, cells were treated with 40 μM Dox for 0, 6, 12, and 24 hours. Previous findings confirmed that CALR protein levels were significantly reduced in HMC3 cells following a 12-hour treatment with 40 μM Dox.[18]

To determine whether the observed changes in CALR levels occurred at the transcriptional or post-translational level, *CALR* mRNA expression was assessed using RT-qPCR. The results indicated that *CALR* mRNA expression in the 12-

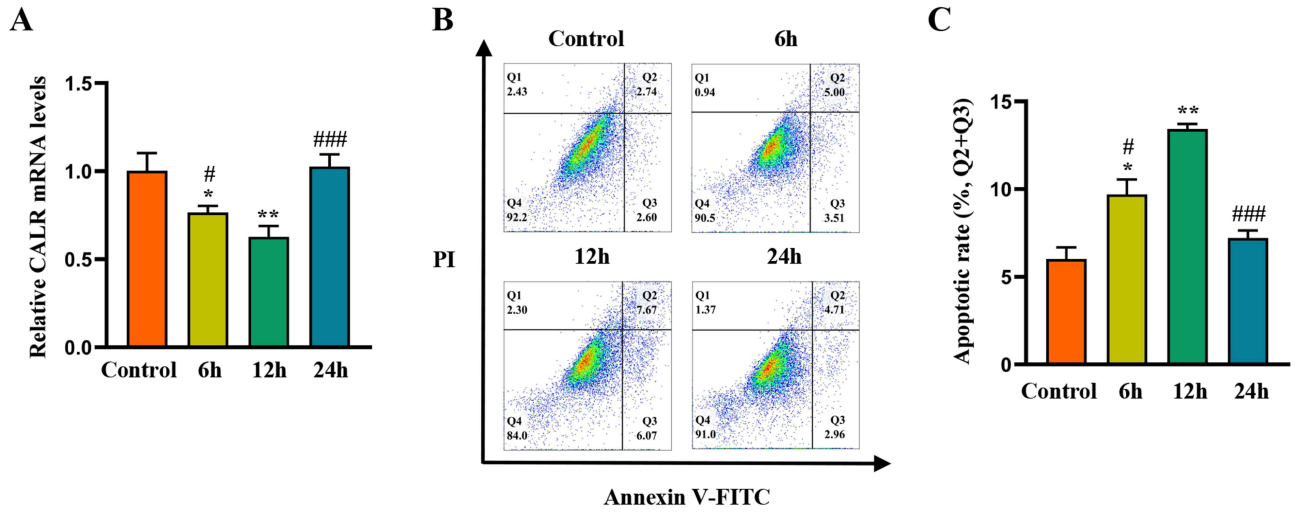

Figure 1 Effects of varying Dox treatment durations on *CALR* expression and HMC3 cell apoptosis. (**A**) Relative *CALR* mRNA expression in each group. (**B**) Flow cytometry analysis of apoptosis in each group. (**C**) Apoptosis rate (percentage of cells in Q2 and Q3) in each group. Results are presented as mean ± standard deviation.
Note: $^{*}p < 0.05$, $^{**}p < 0.01$ versus control; $^{\#}p < 0.05$, $^{\#\#\#}p < 0.001$ versus 12-hour treatment. Experiments were repeated three times independently.

hour treatment group was significantly lower than in the other groups (Figure 1A). Since CALR plays a regulatory role in apoptosis, flow cytometry was used to analyze the apoptosis level of cells in each group (Figure 1B).[31] Apoptosis levels were significantly higher in the 12-hour treatment group compared to the remaining groups (Figure 1C). These findings indicate that *CALR* expression was inhibited, and apoptosis was induced in HMC3 cells following a 12-hour treatment with 40 μM Dox.

The Impact of Varying Concentrations of Dox on CALR Levels and Apoptosis in HMC3 Cells

Based on the previous experimental findings, the effect of Dox concentration was assessed by treating HMC3 cells with varying concentrations of Dox for 12 hours. A prior study confirmed that CALR protein levels were significantly reduced following treatment with 160 μM Dox.[18] Additionally, RT-qPCR analysis revealed a statistically significant reduction in *CALR* mRNA levels in the 160 μM treatment group compared to the other experimental groups (Figure 2A).

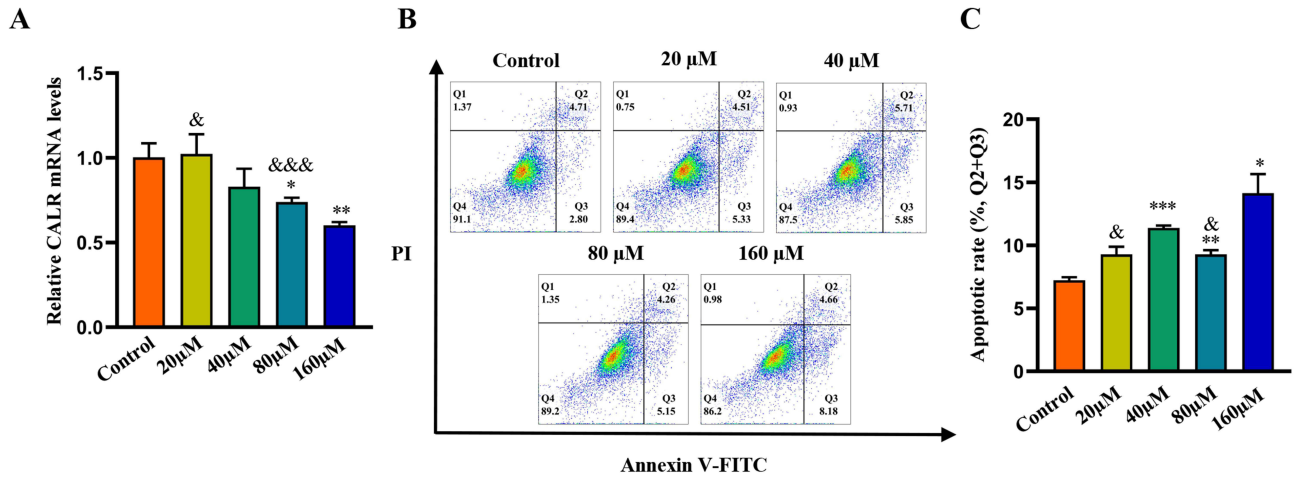

Figure 2 Effects of varying Dox concentrations on apoptosis in HMC3 cells and *CALR* expression. (**A**) RT-qPCR analysis of relative *CALR* mRNA expression in each group. (**B**) Apoptotic rate (percentage of cells in Q2 and Q3) in each group. (**C**) Flow cytometry analysis of apoptosis in different groups. Results are presented as means ± standard deviation.
Note: $^{*}p < 0.05$, $^{**}p < 0.01$, $^{***}p < 0.001$ versus control; $^{\&}p < 0.05$, $^{\&\&\&}p < 0.001$ versus 160 μM. Experiments were performed three times independently.

Apoptosis levels in each group were further evaluated using flow cytometry (Figure 2B), which demonstrated a significant increase in apoptosis in the 40 μM, 80 μM, and 160 μM treatment groups relative to the control group. Among these, the 160 μM group exhibited the highest level of apoptosis (Figure 2C). Previous findings also confirmed that cell viability in the 160 μM treatment group was significantly lower than in the other groups,[18] suggesting that 160 μM Dox exerted some degree of cytotoxicity in HMC3 cells.

Overall, treatment with 160 μM Dox for 12 hours resulted in decreased CALR protein and *CALR* mRNA levels and induced a significant increase in apoptosis.

Dox Inhibits CALR Expression and Elevates Intracellular Free Calcium Concentration in HMC3 Cells

To further confirm the ability of Dox to suppress *CALR* expression, HMC3, *CALR*-overexpressing (*CALR*), and *CALR*-knockdown (sh-*CALR*) cell lines (the latter two constructed in prior experiments) were treated with 160 μM Dox for 12 hours. Cells from each group were harvested, and CALR protein levels were assessed using Western blot analysis (Figure 3A) and RT-qPCR.

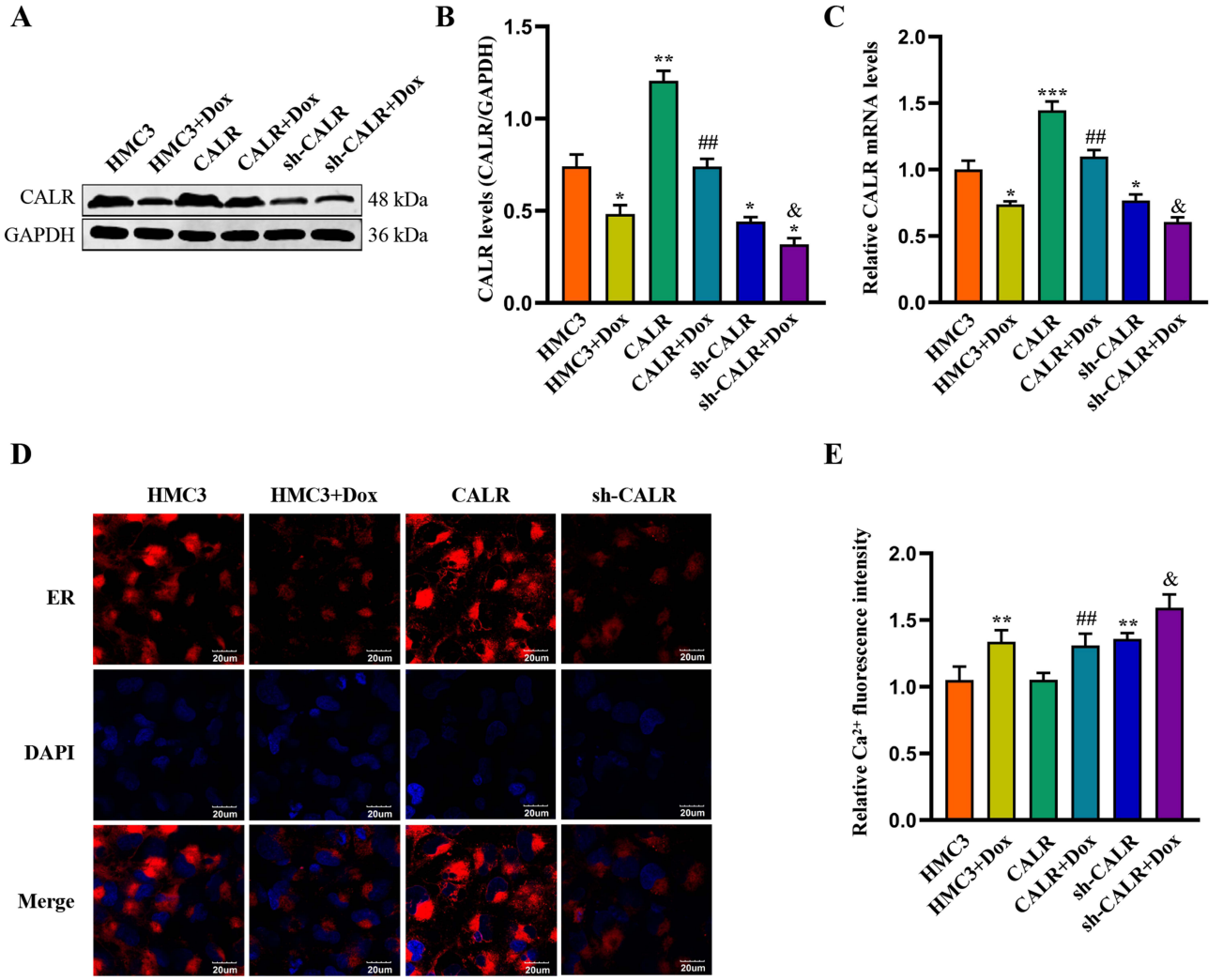

Figure 3 Dox regulates intracellular Ca^{2+} levels and CALR protein expression. (**A**) Western blot analysis of CALR protein expression in each group. (**B** and **C**) Quantification of *CALR* mRNA and CALR protein levels. (**D**) ER tracker fluorescent dye staining of the ER in each group. (**E**) Relative fluorescence intensity of intracellular Ca^{2+} in each group. Results are presented as mean ± standard deviation. Experiments were performed three times independently.
Note: $^{*}p < 0.05$, $^{**}p < 0.01$, $^{***}p < 0.001$ versus HMC3, $^{\#\#}p < 0.01$ versus *CALR*, and $^{\&}p < 0.05$ versus sh-*CALR*.

https://doi.org/10.2147/IDR.S507193

Analysis of relative CALR protein and *CALR* mRNA expression revealed that both CALR protein and *CALR* mRNA levels in the HMC3+Dox, *CALR*+Dox, and sh-*CALR*+Dox groups were significantly reduced compared to their respective control groups (Figure 3B and C). Given that CALR is a chaperone protein localized in the ER lumen, ER tracker staining was performed to determine whether changes in CALR levels affected ER integrity.[32] The results demonstrated that fluorescence intensity in the HMC3+Dox and sh-*CALR* groups was significantly reduced compared to the *CALR* and HMC3 groups (Figure 3D).

As CALR possesses Ca^{2+}-binding properties and is involved in ER calcium homeostasis, intracellular free calcium concentration was measured.[33] The results indicated that intracellular Ca^{2+} levels in the sh-CALR group were significantly higher than in the control group. Additionally, intracellular Ca^{2+} levels were significantly increased in each Dox-treated cell line compared to their corresponding control groups (Figure 3E).

Collectively, these findings demonstrate that Dox suppresses CALR protein expression and induce intracellular Ca^{2+} elevation by affecting the ER.

Dox Activates the IRE1/Caspase-12/Caspase-3 Signaling Pathway by Inhibiting CALR Expression, Thereby Inducing Apoptosis in HMC3 Cells

Based on the findings in Dox Inhibits CALR Expression and Elevates Intracellular Free Calcium Concentration in HMC3 Cells, fluorescence intensity in ER-stained cells was reduced following Dox treatment or *CALR* knockdown. Since CALR knockdown has been shown to increase ER stress in cells,[16] and IRE1 is a key receptor in ER stress regulation,[11] the expression levels of key proteins in the IRE1/Caspase-12/Caspase-3 signaling pathway were quantified using Western blot analysis (Figure 4A).

The results demonstrated that, compared to the HMC3 group, the *CALR* group exhibited significantly lower levels of p-IRE1, cleaved Caspase-12, cleaved Caspase-9, and cleaved Caspase-3 proteins. Conversely, these protein levels were elevated in the sh-*CALR* group (Figure 4B–E). Additionally, the expression levels of these four proteins were significantly higher in the HMC3+Dox, *CALR*+Dox, and sh-*CALR*+Dox groups compared to their respective control groups (Figure 4B–E).

Given that Dox is known to induce apoptosis in vitro, apoptosis was assessed in each group using flow cytometry analysis (Figure 4F), and the apoptosis rate was calculated.[27] The results indicated a significant decrease in the percentage of apoptotic cells in the *CALR* group, whereas a notable increase was observed in the sh-*CALR* group compared to the HMC3 group (Figure 4G). Furthermore, apoptosis levels were significantly elevated in the HMC3+Dox, *CALR*+Dox, and sh-*CALR*+Dox groups relative to their respective control groups (Figure 4G).

These findings suggest that Dox induces apoptosis in HMC3 cells via activation of the IRE1/Caspase-12/Caspase-3 signaling pathway, concomitant with the suppression of CALR protein expression.

Dox Inhibits CALR Expression and Elevates Intracellular Free Calcium Concentration in HMC3 Cells Infected With B. suis S2

Previous research demonstrated that infection of HMC3 cells with *B. suis* S2 at an MOI of 50 for 2 hours significantly inhibited apoptosis in these cells.[18] To further investigate the effects of Dox in this context, HMC3 cells were infected with *B. suis* S2 (MOI = 50) for 2 hours, followed by treatment with 160 μM Dox for 12 hours. Western blot analysis was then performed to assess CALR protein levels (Figure 5A).

Quantification of relative CALR protein expression revealed a significant increase in the HMC3+S2 (2 hours) group, whereas a notable reduction was observed in both the HMC3+Dox and HMC3+S2+Dox groups compared to the HMC3 group. Additionally, CALR levels in the HMC3+S2+Dox group were significantly higher than those in the HMC3+Dox group (Figure 5B).

These trends in *CALR* mRNA expression, assessed via RT-qPCR, were consistent with the protein expression patterns observed in the Western blot analysis (Figure 5C). Also, ER staining indicated that the fluorescence intensity of the ER in both the HMC3+Dox and HMC3+S2+Dox groups was reduced compared to the HMC3 and HMC3+S2 groups (Figure 5D).

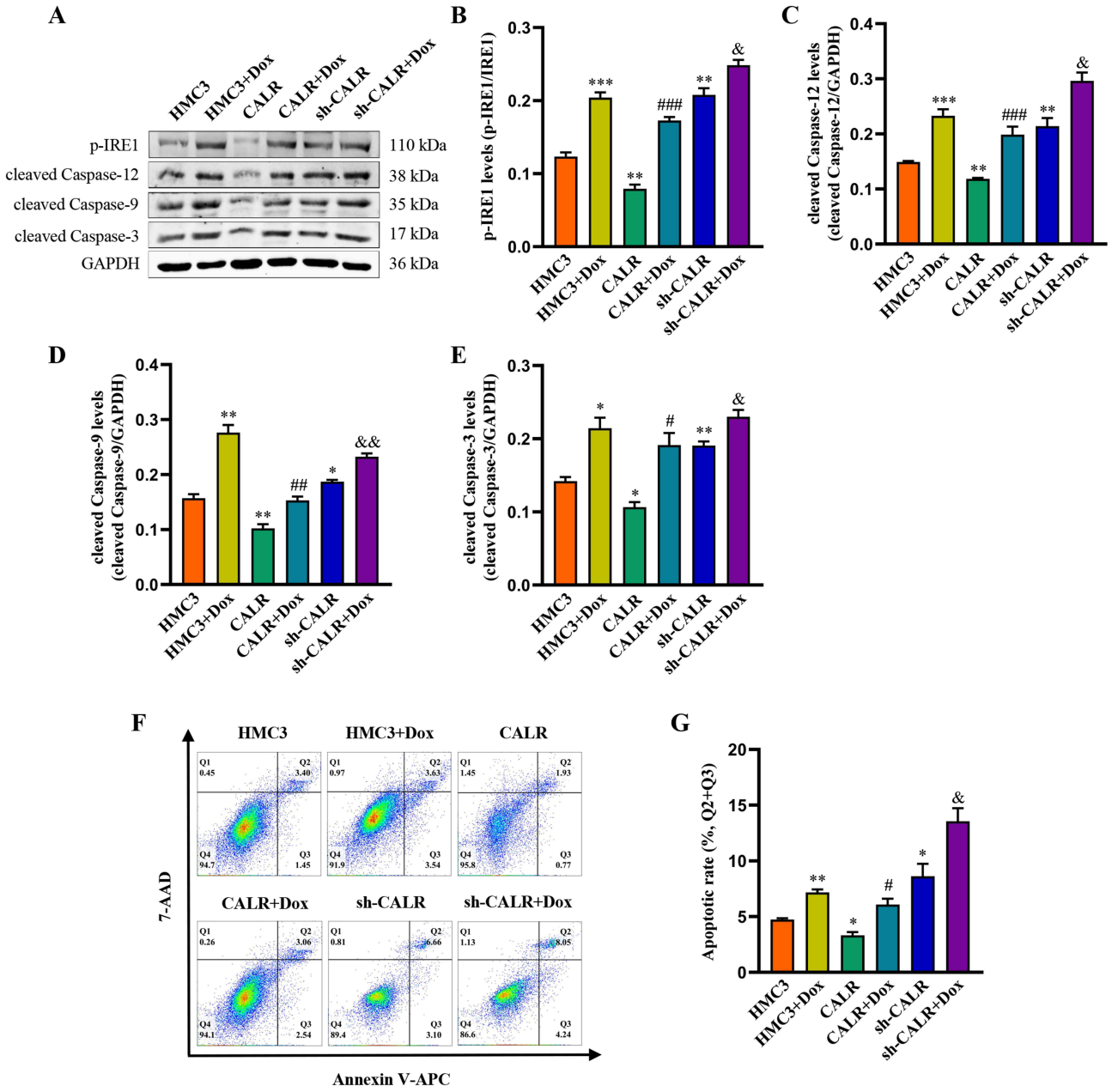

Figure 4 Dox induces apoptosis in HMC3 cells through activation of the IRE1/Caspase-12/Caspase-3 signaling pathway. (**A**) Western blot analysis of key proteins in the IRE1/Caspase-12/Caspase-3 signaling pathway. (**B–E**) Relative protein expression levels of p-IRE1, cleaved Caspase-12, cleaved Caspase-9, and cleaved Caspase-3. (**F**) Flow cytometry analysis of apoptosis in different groups. (**G**) Statistical analysis of the apoptosis rate in each group. Results are presented as mean ± standard deviation. Experiments were performed three times independently.

Note: *$p < 0.05$, **$p < 0.01$, ***$p < 0.001$ versus HMC3, $^{\#}p < 0.05$, $^{\#\#}p < 0.01$, $^{\#\#\#}p < 0.001$ versus *CALR*, and $^{\&}p < 0.05$, $^{\&\&}p < 0.01$ versus sh-*CALR*.

Measurement of intracellular Ca^{2+} fluorescence intensity revealed a substantial increase in intracellular Ca^{2+} levels in both the HMC3+Dox and HMC3+S2+Dox groups compared to the other three groups, with the HMC3+S2+Dox group exhibiting the highest Ca^{2+} concentration (Figure 5E).

These findings indicate that Dox inhibits *CALR* expression and elevates intracellular free calcium concentration in *B. suis* S2-infected HMC3 cells.

https://doi.org/10.2147/IDR.S507193

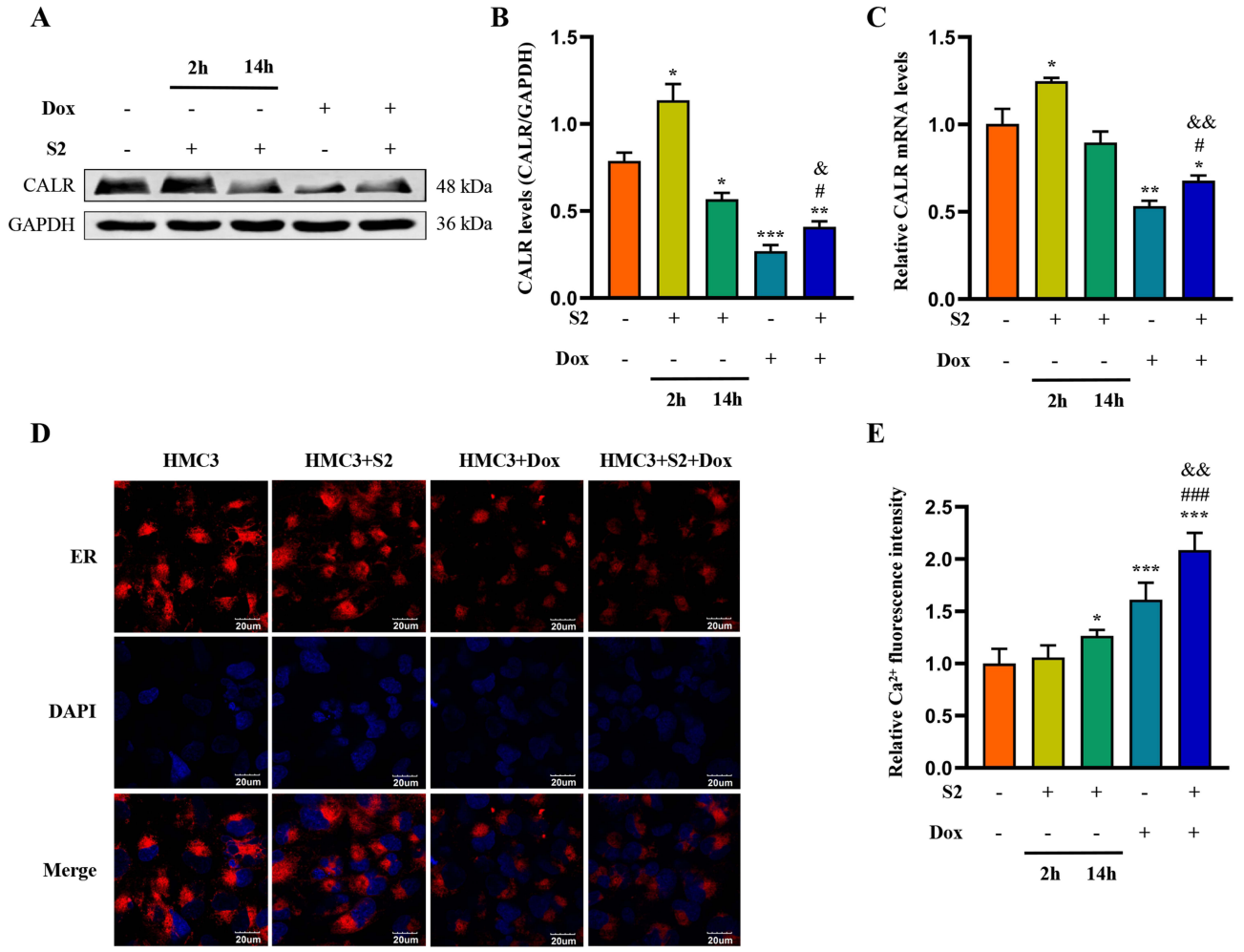

Figure 5 Dox regulates intracellular Ca^{2+} levels and CALR protein expression in *B. suis* S2-infected HMC3 cells. (**A**) Western blot analysis of relative CALR protein expression. (**B**) Densitometric analysis of CALR protein levels. (**C**) RT-qPCR analysis of *CALR* mRNA expression. (**D**) ER fluorescent staining detected by laser confocal microscopy. (**E**) Relative fluorescence intensity of intracellular Ca^{2+} in each group. Results are presented as mean ± standard deviation of three independent experiments. **Note**: $^{*}p < 0.05$, $^{**}p < 0.01$, $^{***}p < 0.001$ versus HMC3; $^{\#}p < 0.05$, $^{\#\#\#}p < 0.001$ versus HMC3+S2 (14 h); $^{\&}p < 0.05$, $^{\&\&}p < 0.01$ versus HMC3+Dox.

Dox Induces Apoptosis in B. suis S2-Infected HMC3 Cells Through Activation of the IRE1/Caspase-12/Caspase-3 Signaling Pathway

Building upon the findings presented in In Vitro Dox Treatment, further investigations were conducted to elucidate the impact of Dox on the IRE1/Caspase-12/Caspase-3 signaling pathway and apoptosis in HMC3 cells infected with *B. suis* S2. Western blot analysis was performed to assess the expression levels of key proteins involved in this pathway (Figure 6A).

Relative densitometry analysis revealed that, compared to the HMC3 group, the expression levels of p-IRE1, cleaved-Caspase12, cleaved-Caspase9, and cleaved-Caspase3 proteins were markedly elevated in the HMC3+S2 (14 hours), HMC3+Dox, and HMC3+S2+Dox groups, whereas these protein levels were significantly reduced in the HMC3+S2 (2 hours) group (Figure 6B–E). Additionally, the expression levels of p-IRE1, cleaved Caspase-9, and cleaved Caspase-3 were significantly higher in the HMC3+S2+Dox group compared to the HMC3+S2 (14 hours) group (Figure 6B–E).

Following cell collection, apoptosis levels were assessed using flow cytometry (Figure 6F). Analysis of apoptotic rates revealed a decrease in apoptosis in the HMC3+S2 (2 hours) group compared to the HMC3 group. In contrast, apoptosis levels were significantly elevated in the HMC3+S2 (14 hours), HMC3+Dox, and HMC3+S2+Dox groups. Notably, the percentage of apoptotic cells in the HMC3+S2+Dox group was significantly higher than in the HMC3+S2 (14 hours) group (Figure 6G).

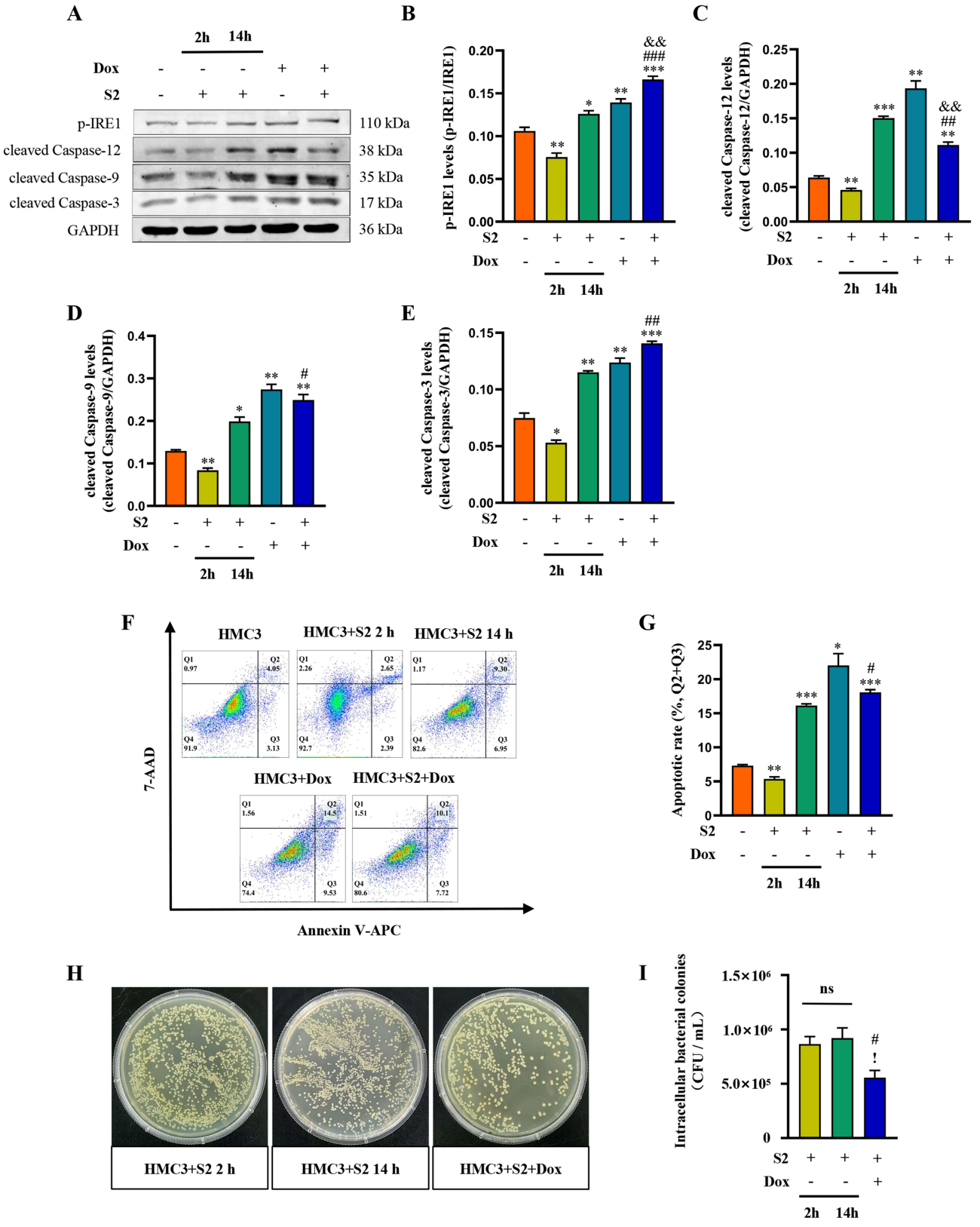

Figure 6 Dox induces apoptosis in *B. suis* S2-infected HMC3 cells through activation of the IRE1/Caspase-12/Caspase-3 signaling pathway. (**A**) Western blot analysis of key proteins in the IRE1/Caspase-12/Caspase-3 signaling pathway. (**B–E**) Quantification of p-IRE1, cleaved Caspase-12, cleaved Caspase-9, and cleaved Caspase-3 protein levels. (**F**) Flow cytometry analysis of apoptosis in different groups. (**G**) Percentage of apoptotic cells in each group. (**H**) Colony formation after culturing cell lysates for 3 days (lysates diluted 100-fold). (**I**) Statistical analysis of intracellular bacterial counts in each group. Results are presented as mean ± standard deviation.

Note: *$p < 0.05$, **$p < 0.01$, ***$p < 0.001$ versus HMC3; $^{\#}p < 0.05$, $^{\#\#}p < 0.01$, $^{\#\#\#}p < 0.001$ versus HMC3+S2 (14 h); $^{\&\&}p < 0.01$ versus HMC3+Dox; $^{!}p < 0.05$ versus HMC3 +S2 (2 h). Each experiment was repeated at least three times.

https://doi.org/10.2147/IDR.S507193

To further investigate the impact of Dox on *B. suis* S2 replication in HMC3 cells, the number of viable intracellular *B. suis* S2 was determined by CFU counting (Figure 6H). The results demonstrated that the number of viable *B. suis* S2 in the HMC3+S2+Dox group was significantly lower than in the other groups, whereas no significant difference was observed between the HMC3+S2 (2 hours) and HMC3+S2 (14 hours) groups (Figure 6I).

In summary, these findings indicate that Dox induces apoptosis in *B. suis* S2-infected HMC3 cells by activating the IRE1/Caspase-12/Caspase-3 signaling pathway and inhibits the replication of *B. suis* S2 in HMC3 cells.

Discussion

Neurobrucellosis, resulting from Brucella infection of the nervous system, constitutes the most severe complication of brucellosis.[34] CNS involvement by *Brucella* presents unique challenges due to its chronic nature and tendency for recurrent episodes.[1] The chronicity and relapses associated with bacterial infection pose unique challenges in the clinical management of neurobrucellosis, primarily due to the ability of *Brucella* to inhibit apoptosis of target cells.[8] Macrophages serve as primary targets of *Brucella* infection, and within the CNS, microglia—the resident macrophages—play a key role in the chronicity of neurobrucellosis.[1] Consequently, there is growing interest in therapeutic strategies aimed at inducing apoptosis in *Brucella*-infected microglia, as this approach holds potential for the treatment of neurobrucellosis.[35]

Dox, a broad-spectrum semi-synthetic tetracycline, has long been established as the preferred therapeutic agent for neurobrucellosis.[36] However, recent attention has shifted towards its non-antibiotic properties, particularly its capacity to induce apoptosis, rather than its conventional bacteriostatic or bactericidal effects.[27] Despite its widespread use, the precise mechanism underlying Dox-induced apoptosis remains completely understood.

In this study, findings indicate that a 12-hour exposure to 160 μM Dox leads to the suppression of *CALR* mRNA expression and the induction of apoptosis in HMC3 cells. Additionally, results demonstrate that treatment with 160 μM Dox induces apoptosis in both uninfected and *B. suis* S2-infected HMC3 cells via activation of the IRE1/Caspase-12/Caspase-3 signaling pathway.

Microglia, the resident macrophages of the CNS, play a critical role in the pathogenesis of neurobrucellosis relapses and chronicity.[6] Given that macrophages are primary targets of *Brucella* infection,[37] the bacterium can modulate microglial function.[6] Upon invading the CNS,[8,18] *Brucella* not only stimulates microglia to release pro-inflammatory factors but also modulates microglial apoptosis. Studies have shown that *Brucella* infection of microglia triggers an inflammatory cascade, characterized by the release of cytokines such as IL-6, IL-1β, and TNF-α, leading to neurological impairment.[1] The present study focuses on understanding the regulatory effects of *Brucella* on microglial activity, which contribute to the persistence and relapse of neurobrucellosis.

Brucella resides within macrophages, forming specialized compartments known as BCVs. The bacterium manipulates the intracellular environment by preventing BCV-lysosome fusion while promoting interactions with the ER.[38] This strategy allows *Brucella* to replicate within the ER and evade macrophage-induced apoptosis.[13] Consequently, inducing apoptosis in *Brucella*-infected microglia via ER-targeted therapeutic strategies is crucial for effective neurobrucellosis treatment, highlighting the need to elucidate the molecular mechanisms involved.

The ER, the largest organelle for protein synthesis and processing in eukaryotic cells, facilitates the maturation of secreted and membrane proteins.[39] Within the ER, chaperone proteins play crucial roles in protein folding and processing.[40] Among these, CALR is a prominent ER chaperone localized in the ER lumen, essential for regulating cellular apoptosis and protein folding.[41] Previous findings confirmed the anti-apoptotic function of CALR,[19] consistent with prior studies. For instance, Sun et al demonstrated the protective role of CALR in adiponectin-mediated myocardial tissue defense against apoptosis,[42] while Jiao et al reported that CALR upregulation conferred resistance to apoptosis in synoviocytes affected by rheumatoid arthritis.[43]

In contrast to these studies, the present research focused on the effects of Dox, a tetracycline antibiotic, on apoptosis in normal or *Brucella*-infected HMC3 cells. Dox is widely recognized for its antibacterial activity against both Gram-positive and Gram-negative bacteria and is the first-line treatment for neurobrucellosis and chronic brucellosis due to its favorable pharmacokinetics and tolerability.[44,45] This study also confirmed that Dox significantly inhibits the replication of *B. suis* S2 in HMC3 cells. However, recent attention has shifted toward its non-antibiotic properties,[27] including its

ability to induce apoptosis and exert immunosuppressive effects.[46] Several studies have demonstrated the apoptosis-inducing effects of Dox in melanoma[27] and breast cancer cell lines.[47] Therefore, this study focused on investigating the apoptotic effects of Dox in *B. suis* S2-infected HMC3 cells.

CALR protein is known to regulate the phagocytic activity of macrophages in infectious diseases.[48] Cockram et al demonstrated that *Escherichia coli* infection enhances microglial phagocytosis by upregulating CALR protein expression,[17] which is consistent with the present observation that *B. suis* S2 infection leads to an upregulation of CALR protein levels in HMC3 cells.

CALR functions as a Ca^{2+}-binding molecular chaperone primarily localized in the ER,[49] where it plays a crucial role in maintaining ER Ca^{2+} homeostasis by modulating Ca^{2+} transport.[50] Based on these findings, this study confirmed that treatment with Dox significantly reduces ER fluorescence intensity and increases intracellular Ca^{2+} levels in both uninfected and *B. suis* S2-infected HMC3 cells. However, *B. suis* S2 infection alone did not induce these effects. The reduction in CALR protein levels following Dox treatment in HMC3 cells disrupts ER structure and leads to the dissociation of bound calcium. This phenomenon is consistent with the findings of Tayyeb et al, where *Calr* knockdown resulted in increased Ca^{2+} levels in mouse kidney cells.[33]

Collectively, these findings underscore the pivotal role of ER homeostasis disruption in mediating Dox-induced apoptosis in both uninfected and *B. suis* S2-infected HMC3 cells.

Building upon the aforementioned results, further investigation was conducted to elucidate the molecular mechanism underlying Dox-induced ER-associated apoptosis in both uninfected and *B. suis* S2-infected HMC3 cells. Bacterial infection or physiological damage can trigger ER stress by causing the accumulation of misfolded or unfolded proteins within the ER,[51] prompting the UPR to reestablish ER homeostasis.[52] External stimuli activate sensor[11] proteins such as IRE1, PERK, and ATF6,[11] which initiate the UPR to alleviate ER stress. Among these sensors, IRE1 IRE1 is particularly pivotal as it is the most conserved ER stress sensor and plays a crucial role in modulating host cell apoptosis during bacterial infection.[53]

Our findings confirm that *B. suis* S2 inhibits the activation of the IRE1 protein and subsequently suppresses apoptosis in HMC3 cells. This observation aligns with the study by Zhi et al, which demonstrated that *B. suis* S2 inhibited apoptosis in goat trophoblasts by suppressing the IRE1-mediated UPR.[54] Similarly, previous reports have shown that *B. suis* 1330 can inhibit apoptosis in human monocytes to facilitate its intracellular survival.[55] Notably, while those studies primarily focused on the IFN-γ apoptotic pathway, our investigation centers on ER stress-associated apoptosis. Conversely, Byndloss et al reported that *B. abortus* induced placental trophoblast apoptosis through activation of the IRE1 pathway,[55] suggesting that discrepancies among findings may be attributed to differences in bacterial strains and cell lines employed.

Activated IRE1 can subsequently activate Caspase-12,[13] which serves as an initiator of the ER stress response and is exclusively activated during ER stress.[56] Activated Caspase-12 then triggers downstream Caspase-9 and Caspase-3, ultimately culminating in apoptosis.[57] Our results demonstrate that *B. suis* S2 sequentially suppresses the activation of Caspase-12, Caspase-9, and Caspase-3, thereby inhibiting HMC3 cell apoptosis. This finding is consistent with the study by Zhi et al, which reported the inhibition of Caspase-3-dependent apoptosis in trophoblast cells by *B. suis* S2.[54]

In light of these results, targeting the IRE1/Caspase-12/Caspase-3 signaling pathway with pharmacological agents appears to be a promising strategy for the treatment of neurobrucellosis. Furthermore, we investigated the regulatory effects of Dox on ER stress. Prior studies have revealed that Dox induces apoptosis in human skin melanoma cells by activating caspases[27] and leads to ER expansion by inducing ER stress.[28] Although the precise molecular mechanisms underlying Dox-induced apoptosis and ER stress remain elusive, our study provides additional evidence that Dox induces apoptosis in both normal and *B. suis* S2-infected HMC3 cells via activation of the IRE1/Caspase-12/Caspase-3 signaling pathway. This finding refines the mechanism by which Dox induces apoptosis.

Our study demonstrated that *B. suis* S2 inhibits the IRE1/Caspase-12/Caspase-3 signaling pathway by upregulating CALR expression. More importantly, this study verified that Dox induces activation of the IRE1/Caspase-12/Caspase-3 signaling pathway through the suppression of CALR protein levels, thereby promoting apoptosis in both uninfected and *B. suis* S2-infected HMC3 cells. A major limitation of this study is the lack of in vivo verification of this mechanism,

which warrants further investigation. Additionally, identifying the precise molecular target of Dox on the CALR protein would provide valuable insights for future research.

Conclusion

These findings elucidate the mechanism by which Dox induces apoptosis in *B. suis* S2-infected HMC3 cells, specifically through the reduction of CALR levels and activation of the IRE1/Caspase-12/Caspase-3 pathway. This study highlights potential therapeutic targets for clinical intervention in neurobrucellosis. In particular, the observed changes in CALR levels and its regulation of ER stress-associated proteins provide new insights for identifying effective drugs that interact with this pathway. These findings serve as a foundation for the development of pharmacological treatments for neurobrucellosis.

Abbreviations

Dox, Doxycycline*B. suis* S2, B*rucella suis* S2 strain: HMC3, Human microglial clone 3: CALR, Calreticulin: RT-qPCR, Real-time quantitative polymerase chain reaction: IRE1, Inositol-requiring enzyme-1: ER, Endoplasmic reticulum: CNS, Central nervous system: BCV, Brucella-containing vacuoles: UPR, Unfolded protein response: PERK, PKR-like ER kinase: ATF6, Activating transcription factor-6: STR, Short tandem repeat: DMEM, Dulbecco's modified Eagle medium: FBS, Fetal bovine serum: PBS, Phosphate-buffered saline: MOI, Multiplicity of infection: SDS, Sodium dodecyl sulfate: PVDF, Polyvinylidene difluoride: TBST, Tris-buffered saline with 0.1% Tween: MOD, Mean optical densities: Tm, Temperatures: PI, Propidium iodide: HBSS, Hank's Balanced Salt Solution: SD, Standard deviation: ANOVA, One-way analysis of variance: CFU, Colony Forming Unit.

Data Sharing Statement

The original contributions presented in the study are included in the article. Further inquiries can be directed to the corresponding authors (Qian Yang or Zhen-Hai Wang).

Acknowledgments

We acknowledge Prof. Zhijun Zhao, Ms. Li Zhong, Ms. Xia Qiao, Ms. Yajing Su and Mr. Pengtao Wang from the team of Ningxia Key Laboratory of Clinical Pathogenic Microorganisms (BSL-2 Laboratory) for their critical support on our experimental activities.

Funding

This work was supported by the National Natural Science Foundation of China (grant number 31660030 and 81960233), the Key Program of Natural Science Foundation of China (grant number 31930048), the Key Research and Development Project of Ningxia Hui Autonomous Region (grant number 2019BCG01003), the Clinical Innovation and Treatment Capacity Enhancement Project of the Second Affiliated Hospital of Air Force Medical University (grant number 2022TDLCTS19) and the Science and Technology Program of the Joint Fund of Scientific Research for the Public Hospitals of Inner Mongolia Academy of Medical Sciences (grant number 2023GLLH0428).

Disclosure

The authors declare that the research was conducted in the absence of any commercial or financial relationships that could be construed as a potential conflict of interest.

References

1. Rodríguez AM, Delpino MV, Miraglia MC, et al. Immune mediators of pathology in neurobrucellosis: from blood to central nervous system. *Neuroscience*. 2019;410:264–273. doi:10.1016/j.neuroscience.2019.05.018
2. Miraglia MC, Rodriguez AM, Barrionuevo P, et al. Brucella abortus traverses brain microvascular endothelial cells using infected monocytes as a trojan horse. *Front Cell Infect Microbiol*. 2018;8:200. doi:10.3389/fcimb.2018.00200
3. Soares CN, MTTD S, Lima MA. Neurobrucellosis. *Curr Opin Infect Dis*. 2023;36:192–197. doi:10.1097/QCO.0000000000000920
4. Soares CN, Angelim AIM, Brandão CO, et al. Neurobrucellosis: the great mimicker. *Rev Soc Bras Med Trop*. 2022;55:e05672021. doi:10.1590/0037-8682-0567-2021

5. Borst K, Dumas AA, Prinz M. Microglia: immune and non-immune functions. *Immunity*. 2021;54:2194–2208. doi:10.1016/j.immuni.2021.09.014
6. Rodríguez AM, Delpino MV, Miraglia MC, et al. Brucella abortus-activated microglia induce neuronal death through primary phagocytosis. *Glia*. 2017;65:1137–1151. doi:10.1002/glia.23149
7. Diesselberg C, Ribes S, Seele J, et al. Activin A increases phagocytosis of Escherichia coli K1 by primary murine microglial cells activated by toll-like receptor agonists. *J Neuroinflammation*. 2018;15:175. doi:10.1186/s12974-018-1209-2
8. Guo X, Zeng H, Li M, et al. The mechanism of chronic intracellular infection with Brucella spp. *Front Cell Infect Microbiol*. 2023;13:1129172. doi:10.3389/fcimb.2023.1129172
9. Sedzicki J, Tschon T, Low SH, et al. 3D correlative electron microscopy reveals continuity of Brucella-containing vacuoles with the endoplasmic reticulum. *J Cell Sci*. 2018;131:jcs210799. doi:10.1242/jcs.210799
10. Hetz C, Zhang K, Kaufman RJ. Mechanisms, regulation and functions of the unfolded protein response. *Nat Rev Mol Cell Biol*. 2020;21(8):421–438. doi:10.1038/s41580-020-0250-z
11. Kumar A, Singh PK, Zhang K, et al. Toll-like receptor 2 (TLR2) engages endoplasmic reticulum stress sensor IRE1α to regulate retinal innate responses in Staphylococcus aureus endophthalmitis. *FASEB J*. 2020;34:13826–13838. doi:10.1096/fj.202001393R
12. Ahmed W, Zheng K, Liu ZF. Establishment of chronic infection: Brucella's stealth strategy. *Front Cell Infect Microbiol*. 2016;6:30. doi:10.3389/fcimb.2016.00030
13. Byndloss MX, Tsai AY, Walker GT, et al. Brucella abortus infection of placental trophoblasts triggers endoplasmic reticulum stress-mediated cell death and fetal loss via type IV secretion system-dependent activation of CHOP. *mBio*. 2019;10:e01538–19. doi:10.1128/mBio.01538-19
14. García de la Cadena S, Massieu L. Caspases and their role in inflammation and ischemic neuronal death. focus on caspase-12. *Apoptosis*. 2016;21:763–777. doi:10.1007/s10495-016-1247-0
15. Li H, Zhang X, Qi X, et al. Icariin inhibits endoplasmic reticulum stress-induced neuronal apoptosis after spinal cord injury through modulating the PI3K/AKT signaling pathway. *Int J Biol Sci*. 2019;15:277–286. doi:10.7150/ijbs.30348
16. Massaeli H, Viswanathan D, Pillai DG, et al. Endoplasmic reticulum stress enhances endocytosis in calreticulin deficient cells. *Biochim Biophys Acta Mol Cell Res*. 2019;1866:727–736. doi:10.1016/j.bbamcr.2018.12.003
17. Cockram TOJ, Puigdellívol M, Brown GC. Calreticulin and galectin-3 opsonise bacteria for phagocytosis by microglia. *Front Immunol*. 2019;10:2647. doi:10.3389/fimmu.2019.02647
18. Wang Z, Wang Y, Yang H, et al. Doxycycline induces apoptosis of Brucella suis S2 strain-infected HMC3 microglial cells by activating calreticulin-dependent JNK/p53 signaling pathway. *Front Cell Infect Microbiol*. 2021;11:640847. doi:10.3389/fcimb.2021.640847
19. Wang Z, Wang Y, Yang S, et al. Brucella suis S2 strain inhibits IRE1/caspase-12/caspase-3 pathway-mediated apoptosis of microglia HMC3 by affecting the ubiquitination of CALR. *mSphere*. 2025;10(3):e0094124. PMID: 40019270; PMCID: PMC11934333. doi:10.1128/msphere.00941-24
20. Ding J, Pan Y, Jiang H, et al. Whole genome sequences of four Brucella strains. *J Bacteriol*. 2011;193:3674–3675. doi:10.1128/jb.05155-11
21. Liu Z, Wang M, Tian Y, et al. A systematic analysis of and recommendations for public health events involving brucellosis from 2006 to 2019 in China. *Ann Med*. 2022;54:1859–1866. doi:10.1080/07853890.2022.2092894
22. Li J, Zhang G, Zhi F, et al. BtpB inhibits innate inflammatory responses in goat alveolar macrophages through the TLR/NF-κB pathway and NLRP3 inflammasome during Brucella infection. *Microb Pathog*. 2022;166:105536. doi:10.1016/j.micpath.2022.105536
23. Zhai Y, Fang J, Zheng W, et al. A potential virulence factor: Brucella flagellin FliK does not affect the main biological properties but inhibits the inflammatory response in RAW264.7 cells. *Int Immunopharmacol*. 2024;133:112119. doi:10.1016/j.intimp.2024.112119
24. Park JA, Pineda M, Peyot ML, et al. Degradation of oxytetracycline and doxycycline by ozonation: degradation pathways and toxicity assessment. *Sci Total Environ*. 2023;856:159076. doi:10.1016/j.scitotenv.2022.159076
25. Głowacka P, Żakowska D, Naylor K, et al. Brucella – virulence factors, pathogenesis and treatment. *Pol J Microbiol*. 2018;67:151–161. doi:10.21307/pjm-2018-029
26. Li YA, Chen HY, Hsieh CP, et al. Acute generation of reactive oxygen species that induced by doxycycline pretreatment results in rapid cell death in polyphyllin G-treated osteosarcoma cell lines. *Environ Toxicol*. 2023;38:1174–1184. doi:10.1002/tox.23757
27. Rok J, Karkoszka M, Rzepka Z, et al. Cytotoxic and proapoptotic effect of doxycycline - an in vitro study on the human skin melanoma cells. Toxicol. *Vitro*. 2020;65:104790. doi:10.1016/j.tiv.2020.104790
28. Spaan CN, Smit WL, van Lidth de Jeude JF, et al. Expression of UPR effector proteins ATF6 and XBP1 reduce colorectal cancer cell proliferation and stemness by activating PERK signaling. *Cell Death Dis*. 2020;10:490. doi:10.1038/s41419-019-1729-4
29. Matsumoto T, Uchiumi T, Monji K, et al. Doxycycline induces apoptosis via ER stress selectively to cells with a cancer stem cell-like properties: importance of stem cell plasticity. *Oncogenesis*. 2017;6:397. doi:10.1038/s41389-017-0009-3
30. Alexander-Savino CV, Hayden MS, Richardson C, et al. Doxycycline is an NF-kappa b inhibitor that induces apoptotic cell death in malignant T-cells. *Oncotarget*. 2016;7:75954–75967. doi:10.18632/oncotarget.12488
31. Wang X, Liu X, Chen Y, et al. Calreticulin regulated intrinsic apoptosis through mitochondria-dependent and independent pathways mediated by ER stress in arsenite exposed HT-22 cells. *Chemosphere*. 2020;251:126466. doi:10.1016/j.chemosphere.2020.126466
32. Michalak M, Groenendyk J, Szabo E, et al. Calreticulin, a multi-process calcium-buffering chaperone of the endoplasmic reticulum. *Biochem J*. 2009;417:651–666. doi:10.1042/BJ20081847
33. Tayyeb A, Dihazi GH, Tampe B, et al. Calreticulin shortage results in disturbance of calcium storage, mitochondrial disease, and kidney injury. *Cells*. 2022;11:1329. doi:10.3390/cells11081329
34. Guven T, Ugurlu K, Ergonul O, et al. Neurobrucellosis: clinical and diagnostic features. *Clin Infect Dis*. 2022;56:1407–1412. doi:10.1093/cid/cit072
35. Yagupsky P, Morata P, Colmenero JD. Laboratory diagnosis of human Brucellosis. *Clin Microbiol Rev*. 2019;33(1):e00073–19. doi:10.1128/CMR.00073-19
36. Jiang H, O'Callaghan D, Ding JB. Brucellosis in China: history, progress and challenge. *Infect Dis Poverty*. 2020;9:55. doi:10.1186/s40249-020-00673-8
37. Chaves-Olarte E, Guzmán-Verri C, Méresse S, et al. Activation of Rho and Rab GTPases dissociates Brucella abortus internalization from intracellular trafficking. *Cell Microbiol*. 2002;4:663–676. doi:10.1046/j.1462-5822.2002.00221.x
38. Celli J, Chastellier C, Franchini DM, et al. Brucella evades macrophage killing via VirB-dependent sustained interactions with the endoplasmic reticulum. *J Exp Med*. 2003;198:545–556. doi:10.1084/jem.20030088

39. Wiseman RL, Mesgarzadeh JS, Hendershot LM. Reshaping endoplasmic reticulum quality control through the unfolded protein response. *Mol Cell*. 2022;82:1477–1491. doi:10.1016/j.molcel.2022.03.025
40. Ye J, Liu X. Interactions between endoplasmic reticulum stress and extracellular vesicles in multiple diseases. *Front Immunol*. 2022;13:955419. doi:10.3389/fimmu.2022.955419
41. Wang WA, Groenendyk J, Michalak M. Calreticulin signaling in health and disease. *Int J Biochem Cell Biol*. 2012;44:842–846. doi:10.1016/j.biocel.2012.02.009
42. Sun Y, Zhao D, Yang Y, et al. Adiponectin exerts cardioprotection against ischemia/reperfusion injury partially via calreticulin mediated anti-apoptotic and anti-oxidative actions. *Apoptosis*. 2017;22:108–117. doi:10.1007/s10495-016-1304-8
43. Jiao Y, Ding H, Huang S, et al. Bcl-XL and Mcl-1 upregulation by calreticulin promotes apoptosis resistance of fibroblast-like synoviocytes via activation of PI3K/Akt and STAT3 pathways in rheumatoid arthritis. *Clin Exp Rheumatol*. 2018;36:841–849.
44. Han CH, Park HD, Kim SB, et al. Oxidation of tetracycline and oxytetracycline for the photo-Fenton process: their transformation products and toxicity assessment. *Water Res*. 2020;172:115514. doi:10.1016/j.watres.2020.115514
45. Pellegrini JM, Gorvel JP, Mémet S. Immunosuppressive mechanisms in Brucellosis in light of chronic bacterial diseases. *Microorganisms*. 2020;10:1260. doi:10.3390/microorganisms10071260
46. Paris JL, Villaverde G, Gómez-Graña S, et al. Nanoparticles for multimodal antivascular therapeutics: dual drug release, photothermal and photodynamic therapy. *Acta Biomater*. 2020;101:459–468. doi:10.1016/j.actbio.2019.11.004
47. Chen YF, Yang YN, Chu HR, et al. Role of Integrin αvβ3 in doxycycline-induced anti-proliferation in breast cancer cells. *Front Cell Dev Biol*. 2022;10:829788. doi:10.3389/fcell.2022.829788
48. Feng M, Marjon KD, Zhu F, et al. Programmed cell removal by calreticulin in tissue homeostasis and cancer. *Nat Commun*. 2018;9:3194. doi:10.1038/s41467-018-05211-7
49. Liu N, Li X, Fu Y, et al. Inhibition of lung cancer by vitamin D depends on downregulation of histidine-rich calcium-binding protein. *J Adv Res*. 2020;29:13–22. doi:10.1016/j.jare.2020.08.013
50. Bibi A, Agarwal NK, Dihazi GH, et al. Calreticulin is crucial for calcium homeostasis mediated adaptation and survival of thick ascending limb of Henle's loop cells under osmotic stress. *Int J Biochem Cell Biol*. 2011;43:1187–1197. doi:10.1016/j.biocel.2011.04.012
51. Yu L, Zhang Z, Zou Y, et al. Next-generation sequencing in the diagnosis of neurobrucellosis: a case series of eight consecutive patients. *Ann Clin Microbiol Antimicrob*. 2023;22:44. doi:10.1186/s12941-023-00596-w
52. Chen X, Shi C, He M, et al. Endoplasmic reticulum stress: molecular mechanism and therapeutic targets. *Signal Transduct Target Ther*. 2023;8:352. doi:10.1038/s41392-023-01570-w
53. Choi JA, Song CH. Insights into the role of endoplasmic reticulum stress in infectious diseases. *Front Immunol*. 2020;10:3147. doi:10.3389/fimmu.2019.03147
54. Zhi F, Zhou D, Bai F, et al. VceC mediated IRE1 pathway and inhibited CHOP-induced apoptosis to support Brucella replication in goat trophoblast cells. *Int J Mol Sci*. 2019;20(17):4104. doi:10.3390/ijms20174104
55. Gross A, Terraza A, Ouahrani-Bettache S, et al. In vitro Brucella suis infection prevents the programmed cell death of human monocytic cells. *Infect Immun*. 2000;68:342–351. doi:10.1128/IAI.68.1.342-351.2000
56. Li Y, Yan Y, Liu F, et al. Effects of calcium Ionophore A23187 on the apoptosis of hepatic stellate cells stimulated by transforming growth factor-β1. *Cell Mol Biol Lett*. 2018;23:1. doi:10.1186/s11658-017-0063-z
57. Zhang Q, Liu J, Chen S, et al. Caspase-12 is involved in stretch-induced apoptosis mediated endoplasmic reticulum stress. *Apoptosis*. 2016;21:432–442. doi:10.1007/s10495-016-1217-6